**Proceedings of the ASME 2019
International Design Engineering Technical Conferences
and Computers and Information in Engineering Conference
IDETC/CIE2019
August 18-21, 2019, Anaheim, CA, USA**

DETC2019-97557

PROGRAMMABLE KIRIGAMI: CUTTING AND FOLDING IN SCIENCE, TECHNOLOGY AND ARCHITECTURE

Jingyang Liu*,1,4, Grace Chuang2,4, Hun Chun Sang3, Jenny E. Sabin1,4

1Architecture
Cornell University
Ithaca, USA
jl3449@cornell.edu

2Chemical and
Biomolecular Engineering
Cornell University
Ithaca, USA
gc439@cornell.edu

3LuoLabs
Cornell University
Ithaca, USA
dl79@cornell.edu

4Sabin Design Lab
Cornell University
Ithaca, USA
jsabin@cornell.edu

ABSTRACT

This paper investigates the potential of kirigami-folding with the addition of strategically placed cuts at multiple scales through both computational design and physical prototyping. The study develops a novel method and workflow for generating two-dimensional (2D) kirigami patterns developed from doubly curved three-dimensional (3D) surfaces (Inverse process). Corresponding simulations of the kirigami folding motion from 2D pattern to 3D goal shape are presented (Forward process). The workflow is based on a reciprocal feedback loop including computational design, finite element analysis, dynamic simulation and physical prototyping. Extended from previous research on kirigami geometry, this paper incorporates material properties into the folding process and successfully develops active kirigami models from the DNA scale to human scale. The results presented in this paper provide an attractive method for kirigami design and fabrication with a wide range of scales and applications.

Keywords: Kirigami, Origami, Computational Folding, Digital Fabrication, Programmable Matter

1. INTRODUCTION

As part of projects funded by the National Science Foundation in the Sabin Design Lab at Cornell University titled *Cutting and Pasting - Kirigami in Architecture, Technology, and Science*, this paper is one product of ongoing trans-disciplinary research spanning across the fields of architecture, bio-engineering, materials science, electrical and systems engineering, and computer science. Like origami (ori = folding, gami = paper), the origin of kirigami comes from the art of folding paper, but with the addition of cuts and holes. The word comes from the Japanese kiru, “to cut,” a geometric method and process that brings new techniques, algorithms, and processes for the assembly of open, deployable, and adaptive structural elements and architectural surface assemblies. We ask, how might architecture respond ecologically and sustainably whereby buildings behave more like organisms in their built environments. Inspired by this interest, we developed design models that integrate advanced kirigami geometry and biomimetic principles to develop prototypes that adapt to environmental stimuli such as heat, light and human proximity. Built upon previous research on kirigami geometry, we proposed methods to create kirigami patterns from a given input freeform surface and to simulate the folding motion of planar patterns approximating its 3D goal shape (Liu et al, 2018). In addition to geometric analysis, material properties and structure analysis are analyzed in the reciprocal design process. Together, this synthesis of design, material, and kirigami programming generates applications in the form of sheet systems with emergent behavior across multiple length scales from nano (DNA) to human.

2. BACKGROUND

2.1 Surface Flattening

The generation of 2D patterns from a given 3D freeform surface has been widely investigated in computational origami and kirigami as a surface flattening problem. The developable

---

[1] Contact author: Prof. Jenny E. Sabin (jsabin@cornell.edu)

[*] Current affiliation: Code Lab, Carnegie Mellon University, Pittsburgh, USA (jingyanl@andrew.cmu.edu)

3D surface can be achieved from a 2D planar unstretchable surface with folds and cuts, and the method of prescribing folds can be mathematically described (Huffman, 1976). For instance, Demaine and O'Rourke proposed a computational method to approach a 3D shape from a piecewise linear structure (Demaine et al. 2007). Kilian et al proposed an optimization-based computational framework for the design and reconstruction of general developable surfaces with curved folds based on isometric mapping between 3D mesh and 2D pattern (Kilian et al. 2008). To minimize the cut line, Gaussian curvature of the input surface was introduced as a metric to find the shortest path of cutting (Sheffer et al. 2002, Wang et al 2004). These methods geometrically addressed the surface flattening. However, some of the design goals for engineering and design applications remain unsolved. For example, the folding motion is intrinsically not only a question of spatial transformation of faces, but is also closely relevant to physical and material properties. Additionally, fabrication constraints and efficiency are important factors in application, which are not covered in previous studies. In this paper, along with the geometry study, the design requirements aforementioned are taken into consideration and verified with both digital simulation and physical prototyping.

2.2 Kirigami

The combination of cuts and folds in the surface flattening process is known as scientific kirigami. While origami uses the technique of tucking to hide excess material in the final shape, kirigami addresses these limits by removing the material completely, allowing folding without any excess material (Castle et al., 2014). A design paradigm that employs lattice-based kirigami elements was proposed to approach a variety of three-dimensional shapes from a single kirigami pattern (Sussman et. al 2015). The method simplified 2D unflattened patterns by combining origami with cutting and re-gluing techniques, making self-folding possible.

2.3 Self-folding

Self-folding is an important topic in origami and kirigami engineering. Self-folding material can perform in a predefined way to approach a goal state. Prior studies about self-folding have investigated multiple mechanisms triggered by various environmental stimuli such as thermal changes, microwaves or humidity. Peraza-Hernandez et al studied the mechanisms of self-folding actuated by thermal-responsive shape memory alloy wire mesh with variables of mesh wire thickness, mesh wire spacing, thickness of the insulating elastomer layer and heating power (Peraza-Hernandez et al 2013). Shim et al proposed the use of biocompatible bilayer structures for the fabrication of tunable microcapsules based on micro-origami. The folding mechanism is based on anisotropic volume change of a hydrogel bilayer (Shim et al, 2012). Ahmed et al used dielectric elastomer and magneto active elastomer materials to create multi-field responsive structures, which enable the structure to fold and unfold in different ways in response to electric and/or magnetic field (Ahmed et al, 2013). Liu used black ink patterned shrinky-dinky film to fold a planar sheet into a three-dimensional object using unfocused light (Liu, et al, 2012). At macro-scale, Krieg integrated the elastic and hygroscopic behavior of wood as active drivers for programmable folding. The prototype was robotically fabricated as a full scale pavilion to demonstrate the development of an adaptive, lightweight and modular architectural system (Krieg et al, 2013).

3. MATERIALS AND METHODS

To design a kirigami model, it is necessary to determine the crease pattern that will dictate the folds and cut pattern that will define the area to be removed to facilitate folding. This design process can be categorized into two paradigms: 1.) *Inverse* process or how to create a 2D pattern from a given 3D form; and 2.) *Forward* process, which centers on the simulation of the 2D kirigami pattern into the folded 3D form.

3.1 Inverse process

Inverse process investigates the generation of methods to create cutting and folding patterns from a given 3D form. Important design research on the inverse process has been studied in various fields. In Tachi's study, a method is presented for generating a fold pattern based on an arbitrary three-dimensional mesh, which serves as the goal shape and primary input (2010). Collaborators Fabrizio Scarpa and Randall Kamien developed a rule set to create 3D structures from a flat sheet using bending, folding, cutting, and pasting (Castle et al, 2014). The method for inverse kirigami proposed in this paper augments and builds upon Tachi's and Kamien's theoretical research to combine folding and cutting in order to morph a 2D flat paper into an arbitrary three-dimensional shape without excessive materials.

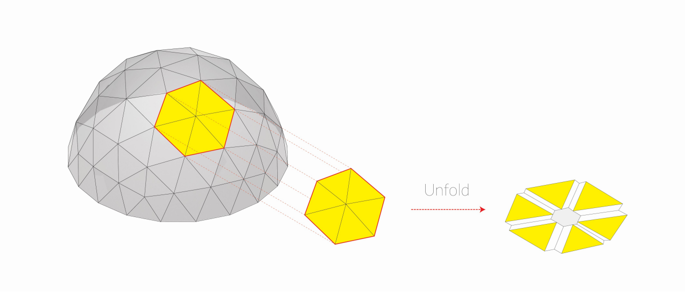

FIGURE 1: Unfold a vertex from given 3D mesh to 2D plane

At the local level, we started by unfolding a polyhedral shape with given Gaussian area from a 3D mesh surface onto 2D plane (Figure 1). The given polyhedral mesh M_0, was initially decomposed into individual polygons and isometrically mapped onto a 2D configuration M_1. Isometric mapping preserves edge lengths and angles of polygons after mapping. Polygons with shared edges are connected by quadrilateral symmetric trapezoid edge molecules which are tucked in to morph the goal mesh M_0 through sequential folding motions. The valley crease is defined by connecting the midpoint of a non-equal edge of the quadrilateral trapezoid edge molecules. The edge molecule is parameterized by two variables corresponding to θ(i,j) and W(i,j) (Figure 2). The θ(i,j), denoting the angle defining by two edges of a molecule, and W(i,j), denoting the width of a molecule, are determined to ensure that the equality and inequality constraints can be satisfied. As for the first equality condition (1), the edge molecule must ensure that mapped polygons associated with each shared vertex forms a closed strip.

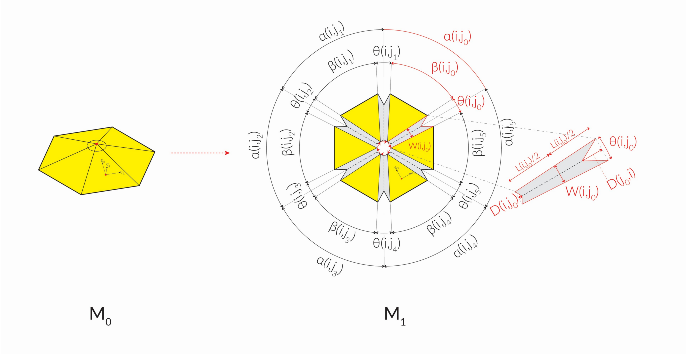

FIGURE 2: Parameterization of 2D planar pattern mapped from a given polyhedral shape

The first equality condition (1) to be met:

$$2\pi = \sum_{n=0}^{N-1} \theta(i, j_n) + \sum_{n=0}^{N-1} \beta(i, j_n) \tag{1}$$

The second equality condition (2) to be met is:

$$\sum_{n=0}^{N-1} w(i, j_n) \begin{bmatrix} \cos\left(\sum_{m=1}^{n} \left(\frac{1}{2}\left(\theta(i, j_{m-1}) + \theta(i, j_m)\right) + \beta(i, j_m)\right)\right) \\ \sin\left(\sum_{m=1}^{n} \left(\frac{1}{2}\left(\theta(i, j_{m-1}) + \theta(i, j_m)\right) + \beta(i, j_m)\right)\right) \end{bmatrix} = \begin{bmatrix} 0 \\ 0 \end{bmatrix} \tag{2}$$

The second equality equation above (2) ensures that vertices of each polygon in 2D pattern M_1 that share the same vertex in the given 3D mesh M_0 form a closed polygon in M_1 (Figure 2). In addition to the equality constraints, inequality constraints (3) need to be incorporated to ensure the edge molecule is valid without overlapping.

$$-\pi < \theta(i, j) < \pi \tag{3}$$

The edge molecule angle value $\theta(i, j)$ must be bounded from -π to π, since the edge molecule will become a straight line if $\theta(i, j)$ reaches ±π.

$$w_{i,j} \geq 0 \tag{4}$$

The second inequality (4) ensures that the exterior fold of an edge molecule must not overlap with the interior fold. The parameter   and   are calculated iteratively until the inequality and equality conditions are met. Based on the value of   and , the translation and rotation vector can be computed to map polygons from the goal mesh to the 2D plane. Between mapped polygons, edge modules with crease lines are created by connecting shared edges of adjacent polygons.

In addition to the crease pattern, the cutting pattern is introduced to avoid edge intersection in the folding motion and reduce material stiffness for self-actuation. To remove the area folded in around each vertex, the major cut is defined by shared vertices of connected polygons. To avoid intersections of the tucked folds, the minor cut which is defined by the angle between adjacent mesh faces and the width of the hinge is applied to the edge molecule (Figure 2).

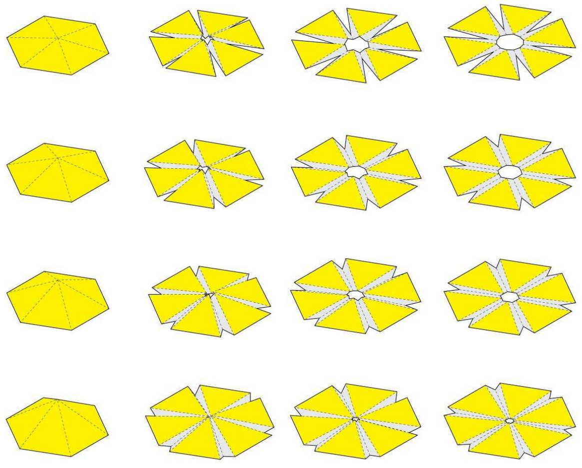

FIGURE 3: Unfolding polyhedral shape with given angle defect

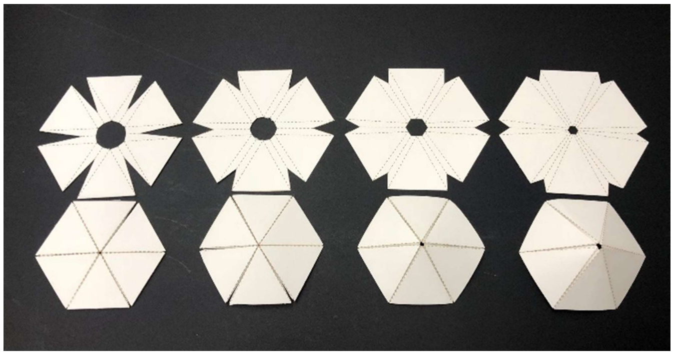

FIGURE 4: Physical prototyping of unfolding polyhedral shape with different angle defect.

As described, a polyhedral shape with given angle defect can be mapped onto a 2D plane by iteratively finding the translation and rotation vectors which meet all equality and inequality conditions through both digital simulation (Figure 3) and physical prototyping (Figure 4). Similarly, an input mesh surface isomorphic to a disc can also be flattened using the same method, since a polyhedral shape can equally represent a vertex of a mesh surface. We then implemented the *inverse* process to unfold a given doubly curved Enneper surface which was initially discretized into a polygonal mesh. All polygons of the mesh were then isometrically mapped onto 2D plane based on translation and rotation vectors that met all constraints of equality and inequality. After mapping, major and minor cuts are applied to remove excessive and overlapping areas in the folding motion. The final 2D pattern was laser-cut with Bristol board ⅛ inch thickness and folded back to the input 3D goal shape. (Figure 5)

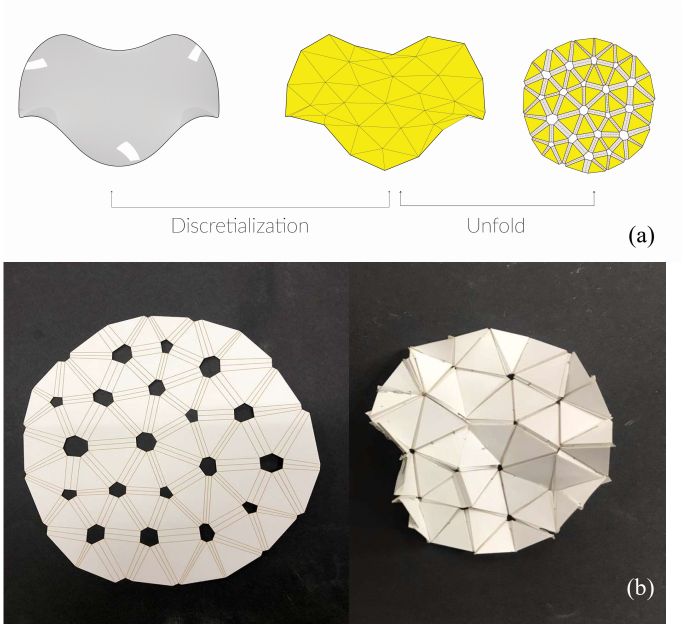

FIGURE 5: (a) Discretization of given Enneper surface and unfold of the surface (Inverse process) (b) Physical prototyping of Enneper surface flattening with Bristol paper board

3.2 Forward process

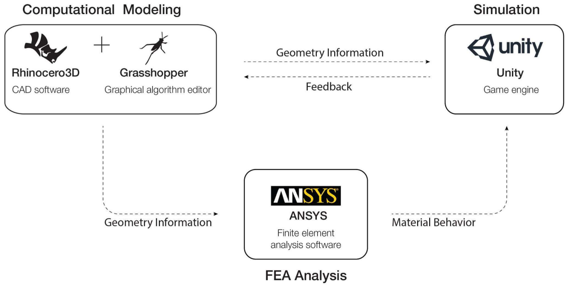

FIGURE 6: Work flow of forward process consists of parametric modeling, finite element analysis and physical simulation

Forward process simulates folding motion from 2D kirigami pattern to 3D form. The simulation method consists of two parts, kinematic analysis evaluating mechanical behavior of folding motion and structural analysis investigating mechanical properties including stress and strain associated with the folding motion. Available mechanical modeling for kinematic analysis include rigid origami folding simulation (Tachi, 2009), finite element method (McGough et al, 2014), the live origami simulator in Kangaroo developed by Daniel Piker. In this paper, we developed and augmented the pin-joint truss framework proposed by Schenk and Guest (Schenk et al, 2011) and constructed a feedback loop between computational modeling, FEA analysis, and dynamic simulation (Figure 6). Information of strain, stress and mechanical energy can be extracted along with the kinematic simulation and used to inform the design of the kirigami pattern. The kinematic analysis that characterizes the geometric transformation of the kirigami unit is based on the dihedral angles and nodal coordinates. The angle between adjacent faces can be calculated from vectors pointing from the folding line towards the nodes of two faces, as shown in Figure 7. The equality constraint shown below is used to find the dihedral angle γ between two adjacent faces from the known vector of three edges connected to the vertex and the value of δ and ε measuring the angle between edges of molecule and the crease line.

$$\sin\gamma = \frac{1}{\sin\delta\sin\varepsilon}\frac{1}{|a|^{3}|b||c|}\big(a\times(c\times a)\big)(a\times b)(5)$$

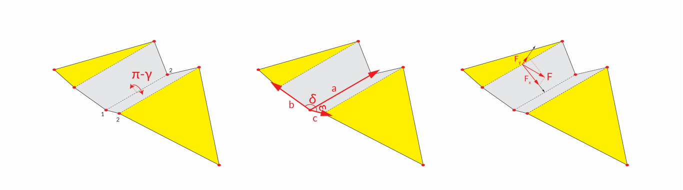

FIGURE 7: The angle between adjacent faces can be calculated based on nodal coordinates of two adjacent faces. The force required to fold two faces depends on the stiffness value K of the fold line.

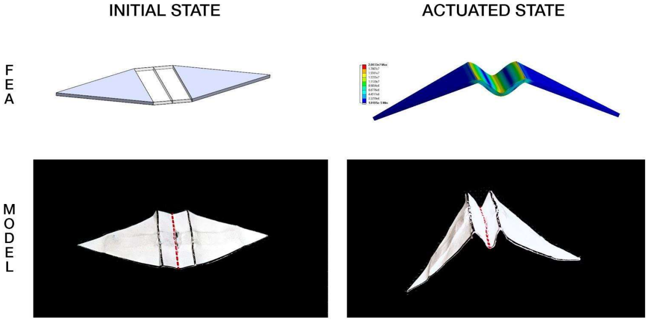

FIGURE 8: Structural analysis of folding motion in the finite element analysis software ANSYS

In addition to kinematic analysis, structural analysis is necessary to estimate the force and energy required for the folding motion, from which, the proper actuation method can be determined. The structural analysis is coupled with kinematic analysis by assigning material stiffness K. The required external force can be calculated by the formula:

$$Kd = Fx \qquad (6)$$

The value of stiffness coefficient K describes the hinge condition, which is relevant to the hinge pattern design and joint type. The increase of the total length of a cut line will weaken the hinge stiffness resulting in the decrease of the K value. The K value will increase if the hinge is reinforced by additional stiff materials like metal and plastic. The structural analysis was implemented in the finite element analysis software ANSYS (Figure 8). The result of structural analysis was output into the game engine Unity 3D as a supplementary information for the simulation of folding motion.

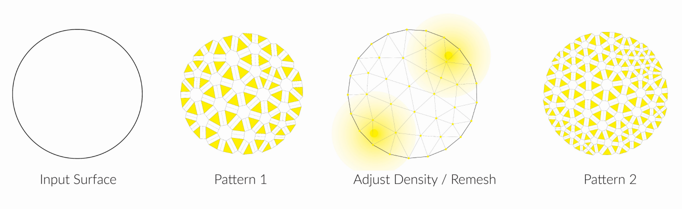

FIGURE 9: User defines boundary and kirigami pattern on 2D plane

The computational design node consists of the geometric modeling tool Rhinocero 3D and the visual programming plugin Grasshopper. The user can define a 2D boundary and create a planar kirigami pattern without manually drawing each face or crease line. Since the generative logic of the kirigami pattern design is encapsulated as a component in Grasshopper, the input parameters are the pattern boundary and tessellation density. By manually increasing or decreasing the local weight of the subdivision level, the density of the kirigami pattern can be modified and varied based on design intention. (Figure 9) The generated 2D pattern was streamed to a FEA analysis and dynamic simulation node, in which the goal shape and the folding motion can be predicted as shown in Figure 10.

With the feedback loop based on the *forward* process, the user can obtain visual feedback and information of structural or kinematic analysis in real-time. The feedback is helpful to guide the design of crease and cutting patterns to provide potential applications for interactive design of kirigami-based products at various scales.

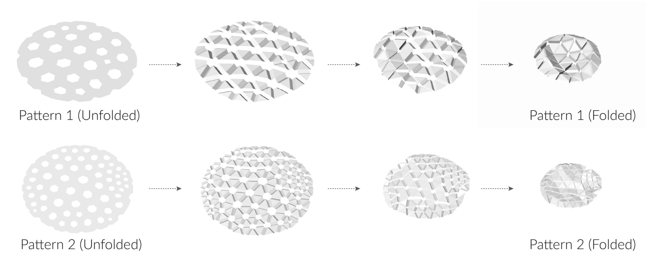

FIGURE 10: The simulation of folding motion from user defined 2D pattern in Unity 3D

4. RESULTS AND DISCUSSION

Based on the proposed interactive design workflow (*inverse* and *forward*), we developed a series of physical prototypes ranging from micro-level to macro-level using materials for actuation like DNA-hydrogel and servos. The design of kirigami products validates our computational design and rationalization approach while also opening up potential applications and use in domains like architecture and bio-molecular engineering.

4.1 Micro-level: DNA Hydrogel kirigami sheet

At the micro and nano-scales, we collaborated with the LuoLabs, in the Department of Biological and Environmental Engineering at Cornell University on developing a simple kirigami design that could be actuated by DNA-Hydrogels.

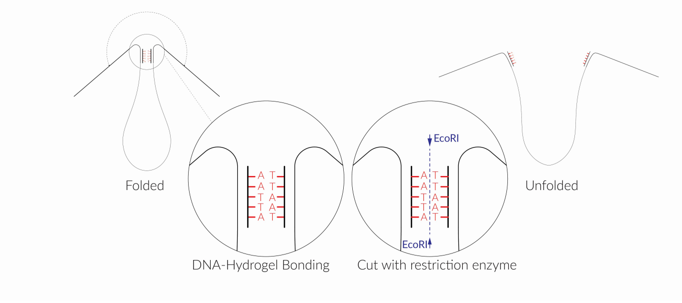

FIGURE 11: DNA-Hydrogel bonded hinge cut by restriction enzyme.

Rolling Chain Amplification (RCA) is an amplification method that replicates a circular DNA template into a long single-stranded DNA molecule. Using RCA, DNA can be non-covalently woven into a hydrogel, driven by the formation of intermolecular I-motifs. The method consists of three steps: annealing, in which the DNA template is mixed with a primer and given time to pair with hydrogen pairing; ligation, in which the DNA template is joined together by ligase, forming a circle; and gelation, in which DNA polymerase replicates the template and primer combination over the course of several days until a viscous liquid is formed.(um et al., 2006)

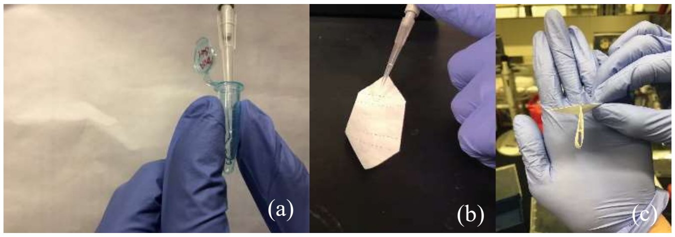

FIGURE 12: (a) DNA-hydrogel preparation (b) Applying DNA-hydrogel to the hinge (c) Tyvek paper hinge bonded by DNA-hydrogel

Since the hydrogel is comprised of DNA, enzymes, such as restriction enzymes, which cleave DNA at specific sequences, or DNase, which degrades DNA by cleaving phosphodiester linkages in the DNA backbone, can be used to release the hydrogel structure. Two or more gels, therefore, can be designed to be cleaved by different restriction enzymes. With this, potential applications of the DNA-Hydrogel actuator include controlled release of specific units within a larger cell structure (Figure 11).

To begin with, we tested subsets of the structure of triangular units. The gel, a viscous material is placed on the hinge part and freeze dried at -80°C. After 2.5 hours in the freezer, we observed the integrity of the design. We found that the gel was strong enough to hold together Tyvek paper, at 14 lb (Figure 12). Then, the enzyme EcoRI was applied to the hinge bonded by the hydrogel. After 1.5 hour, the enzyme cut a specific part of the gel and released the hinge. The mechanism can be applied to a complex matrix consisting of kirigami units bonded by various gel. By choosing restriction enzymes with specific sequences, we can unlock the targeted units and achieve controllable local deformation (Figure 12).

The desired features, like programmable, contextual, and passive unfolding behavior at the nanoscale, enabled by kirigami design and DNA-hydrogel make the composite a promising material used as nano-carriers for targeted delivery.

4.2 Meso-level: Auxetic kirigami sheet

At meso-level, we embedded kirigami geometric rulesets into unstretchable paper board and turned it into an auxetic sheet. Auxetic materials refer to materials with negative poisson ratio. Poisson ratio is a metric describing how a material expands or contracts when being compressed or stretched longitudinally. While for most natural materials, poisson ratio is positive. When they get stretched, most materials will shrink. However, instead of shrinking, auxetic material with positive poisson ratio will expand. Auxetic properties can be found in nature or fabricated with designed geometry. In this paper, we created an auxetic surface based on a geometric design inspired by kirigami pattern.

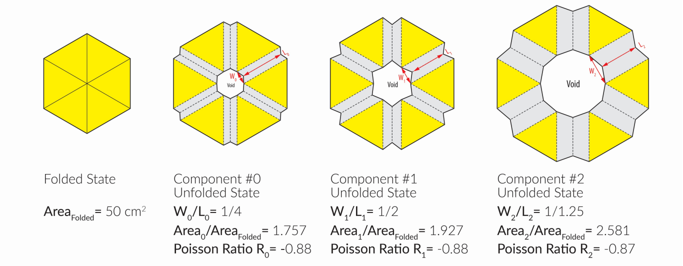

FIGURE 13: Geometric design of the kirigami cell demonstrating the relationship between Poisson ratio and hinge length and width.

The study began by investigating the geometric properties of a kirigami cell. We found that the surface area of the cell with the kirigami pattern increases when the cell is stretched and unfolded. The expansion rate can be measured by the ratio between the surface area of the cell in unfolded and folded status. The study shows that the surface expansion rate depends on the ratio W/L between the width (W) and the length (L) of the edge molecule (Figure 13). As for a single cell, the increase of W/L value results in an increase of the expansion rate. Enabled by geometric design, we can turn conventional analogical materials like paper into auxetic materials.

The model for physical prototyping is made of Bristol paper board substrate of 1/8” thickness and elastic bonding material. The limit of expansion rate is determined by the elongation failure limit of the elastic bonding material. To investigate the relation between the bonding material and expansion rate, we tested and compared two candidates: silicon rubber and synthetic rubber. As for silicon rubber, the limit of strain is 3.9, which means the elongation rate of bonding material must be within the range between 1.0 and 3.9. The range is used as a constraint for the design of the kirigami pattern. As mentioned previously, the expansion rate is correlated with the W/L ratio. From a given range of the expansion rate, the length of each face edge and the parameters of the edge molecule can be determined (Figure 14). By coupling the material property with the computational design of the kirigami cell, a reciprocal feedback was established between the physical model and its digital realms (Figure 15).

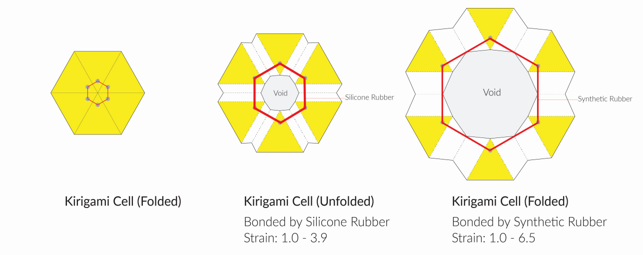

FIGURE 14: Kirigami cell design is based on strain limit of bonding material

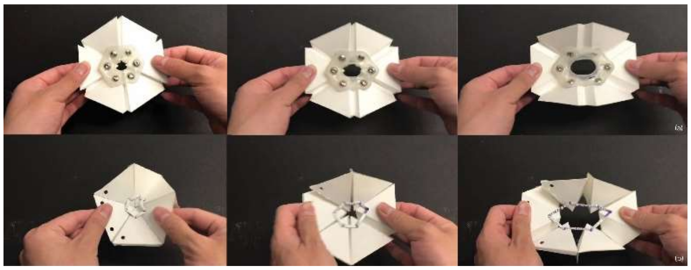

FIGURE 15: Physical prototyping of kirigami cells bonded by silicone rubber and synthetic rubber

Auxetic surface of various expansion rate was created by periodical aggregation of kirigami cells. Arrays of kirigami cells were bonded with elastic synthetic rubber. When the surfaces are stretched under the application of vertical loading at the bottom of the surface, the bonded cells unfold, resulting in the expansion of the surface at a global scale. (Figure 16)

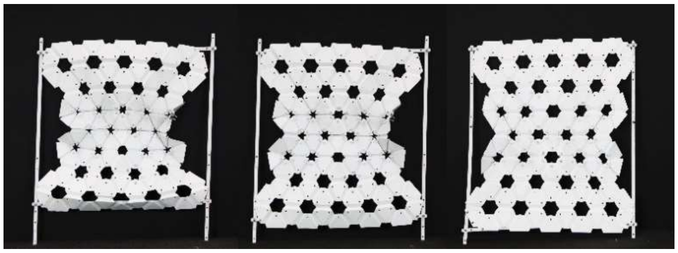

FIGURE 16: Auxetic surface tessellated by kirigami cells expands when it gets pulled down and stretched instead of shrinking.

4.3 Macro-level: Heat-Light responsive kirigami surface

At the macro-level, we developed a heat-light responsive surface by coupling the kirigami geometric rulesets with contextual-responsive actuators. The heat-light responsive surface is tessellated with kirigami modules. The kirigami module consists of five key elements: sensor network, kirigami panel, actuators, microcontroller and a WiFi module (Figure 17). The individual kirigami module is capable of responding to the relative temperature and light of the surrounding environment by folding and unfolding itself. The temperature and light data are extracted from sensors and are synchronized with the digital model in real time via a communication protocol and the WiFi component. The status of the surface is visualized and simulated on a remote computer bridging the gap between the physical and cyber environments. (Figure 18)

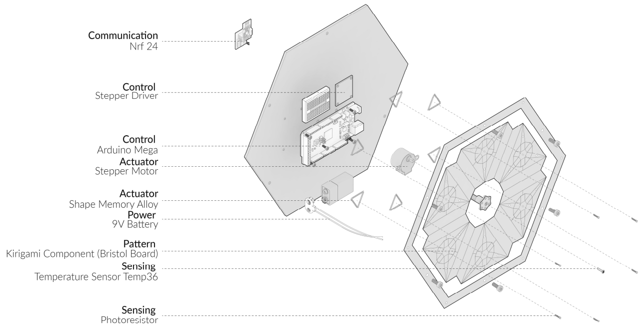

FIGURE 17: Kirigami module consists of sensing, actuation, communication and control layers responding to light and heat environment

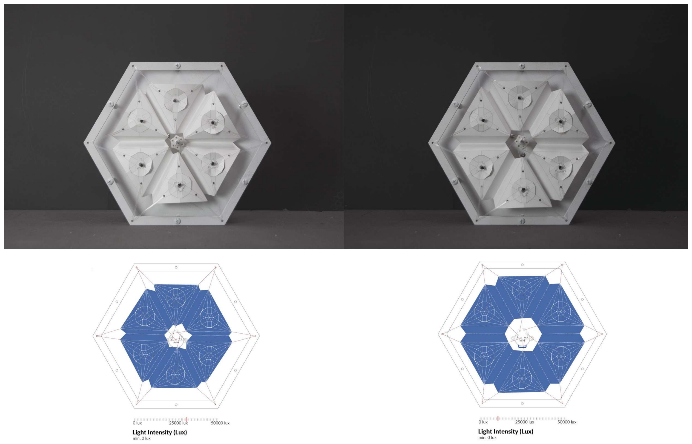

FIGURE 18: Kirigami module responds to light environment by folding and unfolding to increase or turn down the center void, which is synchronized with its digital model.

The sensors for the kirigami module vary from TMP36 temperature sensor used for measuring surrounding temperature to photoresistors used for calibrating daylight. The daylight illuminance data translated from photoresistors are correlated with the stepper's rotation. The stepper rotates and tensions the elastic wire attached to the vertices of the kirigami module. The tension force causes the folding of the module which ends up closing down the center void as a response to the intensity of detected light (Figure 18). At each face of the kirigami module, shape memory alloy (SMA) springs are used as an actuator for out-of-plane folding motion. A SMA is a metallic material that has the ability to recover a given shape when subjected to a suitable thermal cycle. In our case, the SMA is used as an energy-free actuator where the movement is due to the large amount of energy produced by phase changing associated with thermal variations. The spring shrinks when temperature is above 30 Celsius. The 2D pattern folds out of plane and creates cavity for air flux entry (Figure 19). When the temperature is below 15 Celsius, the pattern unfolds and stretches SMA spring with its own rigidity. The thermo-responsive mechanism enabled by SMA guarantees no external power supply is required which makes the module reliable for a sustainable application.

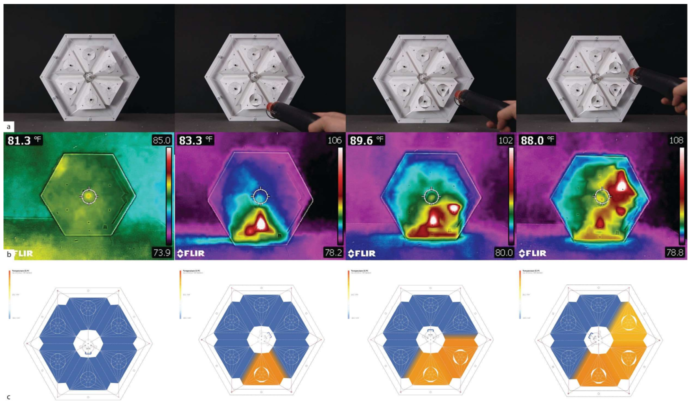

FIGURE 19: Kirigami module responds to heat environment with out-of-plane folding, the thermal image shows the heat distribution over the surface of kirigami module when being heated. The temperature data gathered is visualized and used to predict the folding motion of kirigami module.

The data of temperature and daylight were forwarded to a remote computer via NRF WiFi component and UDP-based customized communication protocol. The data was parsed into numeric format in Processing and used to drive the visualization in model space supported by Rhinoceros and Grasshopper. Through the UDP (User Datagram Protocol), data from the environment and kirigami folding status can be synchronized with the digital model in model space. The parallel coupled relation between virtual and physical world provides an opportunity for a cooperative design method consisting of simulation and physical verification (Figure 20).

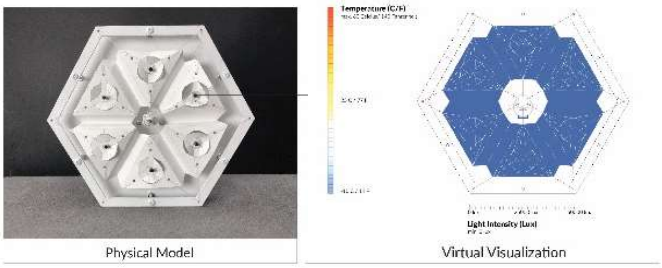

FIGURE 20: The behavior of kirigami module is synchronized with its digital model via wireless communication

The kirigami surface tessellated with kirigami modules is controlled by the decentralized algorithm. Each module is able to respond to the environment stimuli and solve tasks based on its surrounding neighbors. The global response is the result of collective behavior of all kirigami modules. Initially, each module calculates its gradient value defined by light intensity (LI) extracted from photoresistors and folding angle σ_1 ,σ_2 ,σ_3 of three hinges adjacent to the face. The gradient value is defined by $V = LI/(\sigma_1 + \sigma_2 + \sigma_3)$. Then, each module connects with its physically adjacent modules and compares its gradient value with its neighbors. The module of local maximum gradient value becomes the root node and claims its connected modules as a child node. Iteratively, the module of larger gradient value becomes the father node of adjacent modules with smaller value.

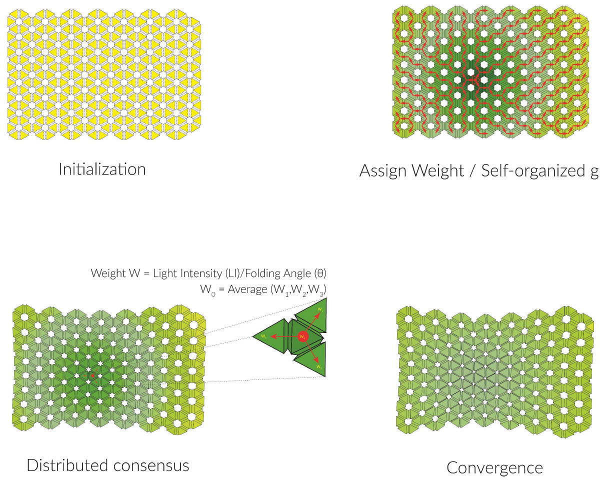

FIGURE 21: Simulation of kirigami surface controlled by the decentralized algorithm

As a result, a tree data structure was constructed based on the gradient value. Modules actuate and fold sequentially from the root node to leaf nodes until the gradient value of each module equals to the average value of its surrounding neighbors. After actuation propagates to the deepest node of the tree, distributed consensus was met and the surface arrived at its equilibrium (Figure 21). Compared to the centralized algorithm, which we assume a central controller stores information of all modules and computes final status, the distributed controlling algorithm is based on local interaction of surrounding modules. Each module is able to undertake a task and respond to stimuli without global control. The algorithm is more reactive and appropriate for uncertain situations, which makes it possible to deploy the thermal-light responsive surface in a variable environment. (Figure 22)

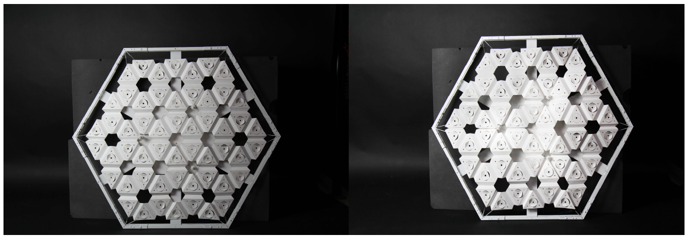

FIGURE 22: Physical prototyping of kirigami surface responding to light intensity

5. CONCLUSION

In this paper, we developed a computational tool to generate 2D kirigami patterns from a general 3D freeform surface (*Inverse* process) and simulate the folding motion from 2D pattern to 3D folded shape (*Forward* process). Alongside the geometric study, metrics relevant to design and fabrication like foldability, density, and complexity were taken into consideration. By creating a workflow that integrates computational modeling, finite element analysis and dynamic simulation, we were able to adjust parameters according to structural analysis and material properties. The results demonstrate the application of programmable kirigami patterns from the micro-scale DNA hydrogel sheet to the macro-scale architectural component via both virtual simulation and physical prototyping. These results demonstrate the scalability of our kirigami design. Regarding actuation, we tested materials from DNA hydrogel to heat responsive shape memory alloy for passive self-folding in response to the local context. As for future exploration, we will focus on creating a synthetic material system integrating both actuation and folding pattern. Manufacturing methods like multi-material additive manufacturing will be explored to fabricate novel synthetic material systems. The material system will include contextual responsive dynamic materials as the actuators and sheet material embedded with kirigami rulesets as the substrate. The kirigami inspired material system will be able to respond to environment stimuli, for instance, thermal, humidity and lighting, in a passive way.

ACKNOWLEDGEMENTS

This material is based upon work supported by the National Science Foundation under grant No. 1331583

Thanks for the support from LuoLabs at Cornell University.

REFERENCES

[1] Liu, Jingyang, Liu, (Chia-Chia) Jasmine, Eggers, Madeleine & Sabin, Jenny E. (2018). “Responsive Kirigami - Context-Actuated Hinges in Folded Sheet Systems.” 22. 10.22360/simaud.2018.simaud.022.

[2] Huffman, David A. "Curvature and creases: A primer on paper." *IEEE Transactions on computers* 10 (1976): 1010-1019.

[3] Kilian, Martin, Simon Flöry, Zhonggui Chen, Niloy J. Mitra, Alla Sheffer, and Helmut Pottmann. "Curved folding." *ACM transactions on graphics (TOG)* 27, no. 3 (2008): 75.

[4] Demaine, Erik D., and Joseph O’Rourke. *Geometric folding algorithms*. Cambridge: Cambridge university press, 2007.

[5] Sheffer, Alla. "Spanning tree seams for reducing parameterization distortion of triangulated surfaces." In *Shape Modeling International, 2002. Proceedings*, pp. 61-272. IEEE, 2002.

[6] Wang, Charlie CL, Yu Wang, Kai Tang, and Matthew MF Yuen. "Reduce the stretch in surface flattening by finding cutting paths to the surface boundary." *Computer-Aided Design* 36, no. 8 (2004): 665-677.

[7] Castle, Toen, Yigil Cho, Xingting Gong, Euiyeon Jung, Daniel M. Sussman, Shu Yang, and Randall D. Kamien. "Making the cut: Lattice kirigami rules." *Physical review letters* 113, no. 24 (2014): 245502.

[8] Sussman, Daniel M., Yigil Cho, Toen Castle, Xingting Gong, Euiyeon Jung, Shu Yang, and Randall D. Kamien. "Algorithmic lattice kirigami: A route to pluripotent materials." *Proceedings of the National Academy of Sciences* 112, no. 24 (2015): 7449-7453.

[9] Peraza-Hernandez, Edwin, Darren Hartl, Edgar Galvan, and Richard Malak. "Design and optimization of a shape memory alloy-based self-folding sheet." *Journal of Mechanical Design*135, no. 11 (2013): 111007.

[10] Shim, Tae Soup, Shin-Hyun Kim, Chul-Joon Heo, Hwan Chul Jeon, and Seung-Man Yang. "Controlled origami folding of hydrogel bilayers with sustained reversibility for robust microcarriers." *Angewandte Chemie International Edition* 51, no. 6 (2012): 1420-1423.

[11] Ahmed, Saad, Carlye Lauff, Adrienne Crivaro, Kevin McGough, Robert Sheridan, Mary Frecker, Paris von Lockette et al. "Multi-field responsive origami structures: Preliminary modeling and experiments." In *ASME 2013 International Design Engineering Technical Conferences and Computers and Information in Engineering Conference*, pp. V06BT07A028-V06BT07A028. American Society of Mechanical Engineers, 2013.

[12] Liu, Ying, Julie K. Boyles, Jan Genzer, and Michael D. Dickey. "Self-folding of polymer sheets using local light absorption." *Soft Matter* 8, no. 6 (2012): 1764-1769.

[13] Krieg, Oliver David, and Achim Menges. "HygroSkin: A climate-responsive prototype project based on the elastic and hygroscopic properties of wood." (2013).

[14] Tachi, Tomohiro. "Origamizing polyhedral surfaces." *IEEE transactions on visualization and computer graphics* 16, no. 2 (2010): 298-311.

[15] Castle, Toen, Yigil Cho, Xingting Gong, Euiyeon Jung, Daniel M. Sussman, Shu Yang, and Randall D. Kamien. "Making the cut: Lattice kirigami rules." *Physical review letters* 113, no. 24 (2014): 245502.

[16] Tachi, Tomohiro. "Simulation of rigid origami." *Origami* 4 (2009): 175-187.

[17] McGough, Kevin, Saad Ahmed, Mary Frecker, and Zoubeida Ounaies. "Finite element analysis and validation of dielectric elastomer actuators used for active origami." *Smart Materials and Structures* 23, no. 9 (2014): 094002.

[18] Schenk, Mark, and Simon D. Guest. "Origami folding: A structural engineering approach." In *Origami 5: Fifth International Meeting of Origami Science, Mathematics, and Education*, pp. 291-304. CRC Press, Boca Raton, FL, 2011.

[19] Um, Soong Ho, Jong Bum Lee, Nokyoung Park, Sang Yeon Kwon, Christopher C. Umbach, and Dan Luo. "Enzyme-catalysed assembly of DNA hydrogel." *Nature materials* 5, no. 10 (2006): 797.